Vortex states in superconducting rings

B. J. Baelus, F. M. Peeters,* and V. A. Schweigert†
Departement Natuurkunde, Universiteit Antwerpen, Universiteitsplein 1, B-2610 Antwerpen, Belgium
(Received 4 October 1999)

The superconducting state of a thin superconducting disk with a hole is studied within the nonlinear Ginzburg-Landau theory in which the demagnetization effect is accurately taken into account. We find that the flux through the hole is not quantized, the superconducting state is stabilized with increasing size of the hole for fixed radius of the disk, and a transition to a multivortex state is found if the disk is sufficiently large. Breaking the circular symmetry through a non-central-location of the hole in the disk favors the multivortex state.

I. INTRODUCTION

Thanks to recent progress in microfabrication and measurement techniques, it is possible to study the properties of superconducting samples with sizes comparable to the penetration depth λ and the coherence length ξ. The properties of these mesoscopic systems are considerably influenced by confinement effects. Therefore, the vortex state will depend on the size and the geometry of the sample.

In the present paper, we study the properties and the vortex states of superconducting thin disks with a hole. In the past, two limiting cases were studied: the thin-wire loop and the disk without a hole. In 1962 Little and Parks studied a thin-wire loop in an axial magnetic field.[1] The T_c-H phase diagram showed a periodic component. Each time a flux quantum $\phi_0=hc/2e$ penetrates the system, $T_c(H)$ exhibits an oscillation. Berger and Rubinstein[2] studied nonuniform mesoscopic superconducting loops using the nonlinear Ginzburg-Landau (GL) theory. They assumed that the induced magnetic field can be neglected for samples with sufficiently small thickness. In the limit of thin loops, the transition between states with different angular momentum L (also called vorticity) occurs when the enclosed flux ϕ equals $(L+1/2)\phi_0$.[3] The superconducting disk was studied by Schweigert *et al.*[4–7] (see also Ref. 8) by solving the two GL equations self-consistently. Although the GL equations were derived to describe superconductivity near the critical point, this theory turns out to be valid over a much broader range of magnetic field and temperature.[7,9] They found that the finite thickness of the disk influences the magnetic field profile, i.e., the magnetic pressure, and this changes the size of the Meissner effect, which is different from the well-studied cylinder geometries.[10] The reverse problem, i.e., the antidot, was studied by Bezryadin *et al.*[11] They obtained a phase diagram of a thin superconducting film with a circular hole in an axial magnetic field by solving numerically the nonlinear GL equations in the limit of a thin film. Here we generalize the results of Ref. 5 to a thin circular superconducting disk containing a circular hole.

The intermediate case of finite width loops was studied previously by Bardeen[12] within the London theory. He showed that in tubes of very small diameter and with wall thickness of the order of the penetration depth the flux through the tube is quantized in units of $\nu\phi_0$, where $\nu<1$ depends on the dimensions of the system. Arutunyan and Zharkov[13,14] found that the flux through the effective area $\pi(\rho^*)^2$ is equal to $m\phi_0$, where the effective radius ρ^* is approximately equal to the geometric mean square of the inner radius R_i and the outer radius R_o of the cylinder; i.e., $\rho^*=(R_iR_o)^{1/2}$. Recently, Fomin *et al.*[15] studied square loops with leads attached to it and found inhomogeneous Cooper-pair distributions in the loop with enhancements near the corners of the square loop. Bruyndoncx *et al.*[16] investigated infinitely thin loops of finite width. In this case, the magnetic field induced by the supercurrents can be neglected and the total magnetic field equals the external applied magnetic field. Furthermore, they used the linearized GL equation, which is only valid near the superconductor/normal boundary where the density of the superconducting condensate $|\psi|^2$ is small. Only the giant vortex state with a definite angular momentum L was studied and they concentrated on the two- (2D) to three-dimensional (3D) crossover. Berger and Rubinstein[17] also studied infinitely thin loops of finite width with broken axial symmetry and they also neglected the induced field.

It is well known that for type-II ($\kappa>1/\sqrt{2}$) superconductors the triangular Abrikosov vortex lattice is energetically favored in the range $H_{c1}<H<H_{c2}$. Since the effective London penetration depth $\Lambda=\lambda^2/d$ increases considerably in thin samples and for $d\ll\lambda$ one would expect the appearance of the Abrikosov multivortex state even in thin rings made with a material with $\kappa<1/\sqrt{2}$. Similar as for the case of a thin disk,[6] we expect that the structure of a finite number of vortices should differ from a simple triangular arrangement in the case of a thin ring and we expect that they will resemble the configurations found for Coulomb clusters, which are confined into a ring.[18]

In the present paper we consider circular flat disks of nonzero width with a circular hole in it, which is not necessary in the center of the disk. The superconducting properties are also studied deep inside the superconducting state where: i) nonlinear effects are important, i.e., $|\psi|$ is not necessarily small, and the nonlinear GL equations have to be solved, ii) the total magnetic field is not homogeneous, i.e., it is spatial varying due to the Meissner effect and the flux quantization condition, which may enhance or diminish the magnetic field through the hole as compared to the applied magnetic field, and iii) due to nonlinear effects the circular symmetric giant

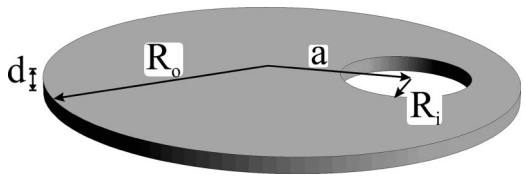

FIG. 1. The configuration: a superconducting disk with radius R_o and thickness d with a hole inside with radius R_i, which is placed a distance a away from the center.

vortex states are not necessarily the lowest energy states and the magnetic field can penetrate the superconductor through single vortices creating a multivortex state.

The paper is organized as follows: In Sec. II we present the theoretical model. In Sec. III we consider a small superconducting disk with a hole in the center. In this case we find that only the giant vortex state appears. We study the influence of the radius of the hole on the superconducting state. For such a small system the relation between the local magnetic field, the current density, and the Cooper-pair density is investigated and the quantization of the flux through the hole is investigated. Next, in Sec. IV, we consider the case of a larger superconducting disk with a hole in the center. For increasing magnetic field, we find re-entrant behavior; i.e., transition from the giant vortex state to the multivortex state and back to the giant vortex state before superconductivity is destroyed. Finally, in Sec. V, we investigate the influence of the position of the hole on the vortex configuration; i.e., what happens if we break the axial symmetry? Our results are summarized in Sec. VI.

II. THEORETICAL FORMALISM

In the present paper, we consider superconducting disks with radius R_o and thickness d with a hole inside with radius R_i, which is placed a distance a away from the center of the disk (Fig. 1). These superconducting ''rings'' are immersed in an insulating medium with a perpendicular uniform magnetic field H_0. To solve this problem we follow the numerical approach of Schweigert and Peeters.[4] For thin disks ($d \ll \xi,\lambda$) they found that it is allowed to average the GL equations over the disk thickness. Using dimensionless variables and the London gauge $div\vec{A}=0$ for the vector potential $\vec{A}$, we write the system of GL equations in the following form

$$(-i\vec{\nabla}_{2D}-\vec{A})^2\Psi=\Psi(1-|\Psi|^2), \tag{1}$$

$$-\Delta_{3D}\vec{A}=\frac{d}{\kappa^2}\delta(z)\vec{j}_{2D}, \tag{2}$$

where

$$\vec{j}_{2D}=\frac{1}{2i}(\Psi^*\vec{\nabla}_{2D}\Psi-\Psi\vec{\nabla}^*_{2D}\Psi)-|\Psi|^2\vec{A} \tag{3}$$

is the density of superconducting current. The superconducting wave function satisfies the following boundary conditions

$$(-i\vec{\nabla}_{2D}-\vec{A})\Psi|_{\vec{r}=\vec{R}_i}=0, \tag{4a}$$

$$(-i\vec{\nabla}_{2D}-\vec{A})\Psi|_{\vec{r}=\vec{R}_o}=0, \tag{4b}$$

and $\vec{A}=\frac{1}{2}H_0\rho\vec{e}_\phi$ far away from the superconductor. Here the distance is measured in units of the coherence length ξ, the vector potential in $c\hbar/2e\xi$, and the magnetic field in $H_{c2}=c\hbar/2e\xi^2=\kappa\sqrt{2}H_c$. The ring is placed in the plane (x,y), the external magnetic field is directed along the z axis, and the indices 2D, 3D refer to two- and three-dimensional operators, respectively.

The giant vortex state in a circular configuration is characterized by the total angular momentum L through $\Psi=\psi(\rho)\exp(iL\phi)$, where ρ and ϕ are the cylindrical coordinates. L is the winding number and gives the vorticity of the system. An arbitrary superconducting state is generally a mixture of different angular harmonics L due to the nonlinearity of the GL equations. Nevertheless, we can introduce an analog to the total angular momentum L, which is still a good quantum number and which is, in fact, nothing else than the number of vortices in the system.

To solve the system of Eqs. (1) and (2), we generalized the approach of Ref. 4 for disks to our fat ring configuration. We apply a finite-difference representation of the order parameter and the vector potential on a uniform Cartesian space grid (x,y), with typically 128 grid points over a distance $2R_o$ (i.e., the diameter of the ring), and use the link variable approach,[19] and an iteration procedure based on the Gauss-Seidel technique to find Ψ. The vector potential is obtained with the fast Fourier transform technique where we set $\vec{A}_{|x|=R_S,|y|=R_S}=H_0(x,-y)/2$ at the boundary of a larger space grid (typically $R_S=4R_o$).

To find the different vortex configurations, which include the metastable states, we search for the steady-state solutions of Eqs. (1) and (2) starting from different randomly generated initial conditions. Then we increase/decrease slowly the magnetic field and recalculate each time the exact vortex structure. We do this for each vortex configuration in a magnetic field range where the number of vortices stays the same. By comparing the dimensionless Gibbs free energies of the different vortex configurations

$$F=V^{-1}\int_V[2(\vec{A}-\vec{A}_0)\cdot\vec{j}_{2d}-|\Psi|^4]d\vec{r}, \tag{5}$$

where integration is performed over the sample volume V, and $\vec{A}_0$ is the vector potential of the uniform magnetic field, we find the ground state. The dimensionless magnetization, which is a direct measure of the expelled magnetic field from the sample, is defined as

$$M=\frac{\langle H\rangle-H_0}{4\pi}, \tag{6}$$

where H_0 is the applied magnetic field. $\langle H\rangle$ is the magnetic field averaged over the sample or detector surface area S.

III. SMALL RINGS: THE GIANT VORTEX STATE

First we discuss a small superconducting ring. Although the system is circular symmetric in general, we are not allowed to assume that $\Psi(\vec{\rho})=F(\rho)e^{iL\theta}$ because of the nonlinear term in the GL equations (1) and (2). Nevertheless, we

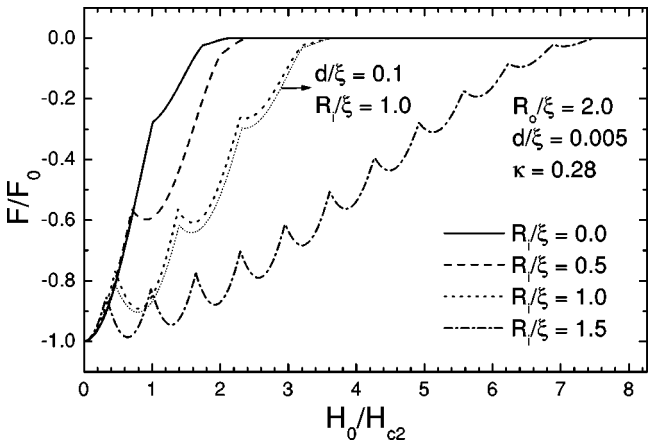

FIG. 2. The ground-state free energy as a function of the applied magnetic field H_0 of a superconducting disk with radius $R_o=2.0\xi$, thickness $d=0.005\xi$, and $\kappa=0.28$ for a hole in the center with radius $R_i/\xi=0.0$, 0.5, 1.0, and 1.5, respectively. The thin dotted curve gives the free energy of a thicker ring with thickness $d=0.1\xi$ and $R_i=1.0\xi$. The free energy is in units of $F_0=H_c^2V/8\pi$.

found that for sufficiently small rings the confinement effects are dominant and this imposes a circular symmetry on the superconducting condensate. If we can assume axial symmetry, the dimensions of the GL equations will be reduced and thus the accuracy and the computation time will be improved. Therefore we will use this method for small rings. For a disk, this kind of solution with fixed L has been called *2D solution* by Deo *et al.*[7] in contrast to the *3D solution* of the general problem.

The ground-state free energy F of a superconducting disk with radius $R_o=2.0\xi$ and thickness $d=0.005\xi$ and GL parameter $\kappa=0.28$ is shown in Fig. 2 for a hole in the center with radius $R_i/\xi=0.0$, 0.5, 1.0, and 1.5, respectively. The situation with $R_i=0$ corresponds to the situation of a superconducting disk without a hole, which was already studied in Ref. 5. With increasing hole radius R_i, we find that the superconducting/normal transition (this is the magnetic field where the free energy equals zero) shifts appreciably to higher magnetic fields and more transitions between different L states are possible before superconductivity disappears. Furthermore, the thin dotted curve gives the free energy for a thicker ring with thickness $d=0.1\xi$ and $R_i=1.0\xi$. In comparison with the previous results for $d=0.005\xi$, the free energy becomes more negative, but the transitions between the different L states occur almost at the same magnetic fields. Thus increasing the thickness of the ring increases superconductivity, which is a consequence of the smaller penetration of the magnetic field into the superconductor.

Experimentally, using magnetization measurements one can investigate the effect of the geometry and the size of the sample on the superconducting state. One of the main advantages of these measurements, in comparison with resistivity measurements, is that they are noninvasive and no conduction probes are needed, which may distort the superconducting state. To investigate the magnetization of a single superconducting disk Geim *et al.*[20] used submicron Hall probes. The Hall cross acts like a magnetometer, where in the ballistic regime the Hall voltage is determined by the average magnetic field through the Hall cross region.[21] Hence, by

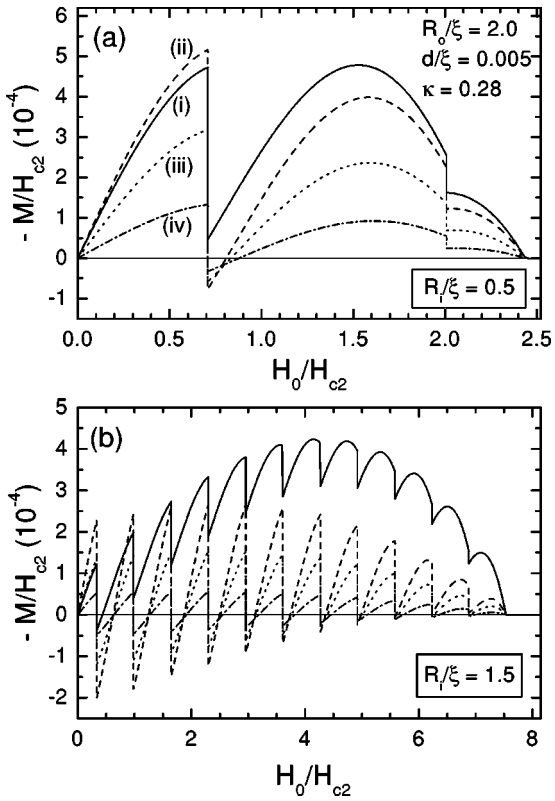

FIG. 3. The magnetization as a function of the applied magnetic field H_0 for a superconducting disk with radius $R_o=2.0\xi$ and thickness $d=0.005\xi$ and $\kappa=0.28$ for a hole in the center with radius $R_i/\xi=0.5$ (a) and $R_i/\xi=1.5$ (b). Curve (i) is the calculated magnetization if we average the magnetic field over the superconducting volume; curve (ii) after averaging the field over the area with radius R_o, i.e., superconductor and hole; curves (iii) and (iv) after averaging the magnetic field over a square region with widths equal to $2R_o$ and $(2+1/2)R_o$, respectively.

measuring the Hall resistance, one obtains the average magnetic field, and, consequently, the magnetic field expelled from the Hall cross [Eq. (6)], which is a measure for the magnetization of the superconductor.[7] As in the case of a superconducting disk,[7] the field distribution in the case of thin superconducting rings is extremely nonuniform inside as well as outside the sample and, therefore, the detector size will have an effect on the measured magnetization. To understand this effect of the detector, we calculate the magnetization for a superconducting ring with outer radius $R_o=2.0\xi$, thickness $d=0.005\xi$, and two values of the inner radius $R_i=0.5\xi$ and $R_i=1.5\xi$ by averaging the magnetic field [see Eq. (6)] over several detector sizes S. The results are shown in Figs. 3(a) and 3(b) as a function of the applied magnetic field for $R_i=0.5\xi$ and $R_i=1.5\xi$, respectively. The solid curve [curve (i)] shows the calculated magnetization if we average the magnetic field over the superconducting volume, and curve (ii) is the magnetization after averaging the field over a circular area with radius R_o, i.e., superconductor and hole. Notice that in the Meissner regime, i.e., $H_0/H_{c2}<0.7$, where $L=0$, the magnetization of superconductor + hole is larger than the one of the superconductor alone, which is due to flux expulsion from the hole. For $L\geqslant 1$ the reverse is true because now flux is trapped in the hole. Experimentally, one usually averages the magnetic field over a

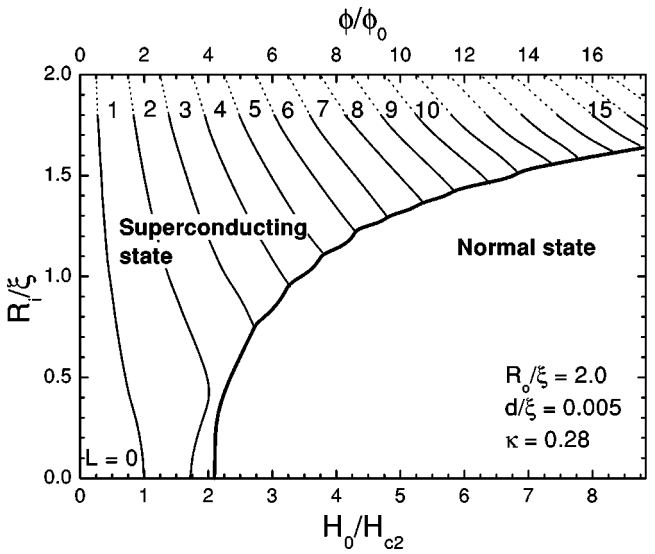

FIG. 4. Phase diagram: the relation between the hole radius R_i and the magnetic fields H_0 at which giant vortex transitions $L \rightarrow L+1$ takes place for a superconducting disk with radius $R_o = 2.0\xi$ and thickness $d = 0.005\xi$ and for $\kappa = 0.28$. The solid curves indicate where the ground state of the free energy changes from one L state to another one and the thick solid curve gives the superconducting/normal transition.

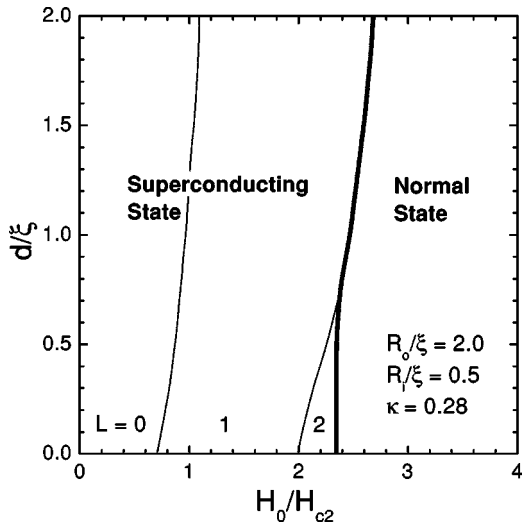

FIG. 5. The same as Fig. 4 but now for varying thickness d of the ring for fixed $R_o = 2.0\xi$, $R_i = 0.5\xi$, and $\kappa = 0.28$.

square Hall cross region. Therefore, we calculated the magnetization by averaging the magnetic field over a square region [curve (iii)] with width equal to $2R_o$, i.e., the diameter of the ring. Curve (iv) shows the magnetization if the sides of the square detector are equal to $(2+1/2)R_o$. Increasing the size of the detector, decreases the observed magnetization because the magnetic field is averaged over a larger region, which brings $\langle H \rangle$ closer to the applied field H_0.

Having the free energies of the different giant vortex configurations for several values of the hole radius varying from $R_i = 0.0\xi$ to $R_i = 1.8\xi$, we construct an equilibrium vortex phase diagram. Figure 4 shows this phase diagram for a superconducting disk with radius $R_o = 2.0\xi$, thickness $d = 0.005\xi$, and for $\kappa = 0.28$. The solid curves indicate where the ground state of the free energy changes from one L state to another and the thick solid curve gives the superconducting/normal transition. The latter exhibits a small oscillatory behavior, which is a consequence of the Little-Parks effect. Notice that the superconducting/normal transition is moving to larger fields with increasing hole radius R_i and more and more flux can be trapped. In the limit $R_i \rightarrow R_o$, the critical magnetic field is infinite and there are an infinite number of L states possible, which is a consequence of the enhancement of surface conductivity for very small samples.[4,22] Because of the finite grid, we were not able to obtain accurate results for $R_i \approx R_o$. The dashed lines connect our results for hole radius $R_i = 1.8\xi$ with the results for $R_i \rightarrow R_o$,[3] where the transitions between the different L states occur when the enclosed flux is $\phi = (L+1/2)\phi_0$, where $\phi_0 = ch/2e$ is the elementary flux quantum. Notice that for rings of nonzero width, i.e., $R_i \neq R_o$, the $L \rightarrow L+1$ transition occurs at higher magnetic field than predicted from the condition $\phi = (L+1/2)\phi_0$. The discrepancy increases with increasing width of the ring and with increasing L. Starting from $R_i = 0$ we find that with increasing R_i the Meissner state disappears at smaller H_0. The hole in the center of the disk allows for a larger penetration of the magnetic field, which favors the $L = 1$ state. This is the reason why the $L = 0 \rightarrow L = 1$ transition moves to a lower external field while the $L = 1 \rightarrow L = 2$ transition initially occurs for larger H_0 with increasing R_i. When the hole size becomes of the order of the width of one vortex the $L = 1 \rightarrow L = 2$ transition starts to move to lower fields and the $L = 2$ state becomes more favorable.

The effect of the thickness of the ring on the phase diagram is investigated in Fig. 5. The thin solid curves indicate where the ground state of the free energy changes from one L state to another one, while the thick curve gives the superconducting/normal transition. Notice that the transition from the $L = 0$ to the $L = 1$ state and the superconducting/normal transition depends weakly on the thickness of the ring. For increasing thickness d, the $L = 2$ state becomes less favorable and disappears for $d \gtrsim 0.7\xi$. In this case, there is a transition from the $L = 1$ state directly to the normal state. Increasing d stabilizes the different L states up to larger magnetic fields. This is due to the increased expulsion of the applied field from the superconducting ring.[4]

In the next step, we investigate three very important and mutually dependent quantities: the local magnetic field H, the Cooper-pair density $|\Psi|^2$, and the current density j. We will discuss these quantities as a function of the radial position ρ. For this study we distinguish two situations, i.e., $R_i \ll R_o$ and $R_i \lesssim R_o$. In the first case the sample behaves more like a superconducting disk, and in the second case like a superconducting loop.

First, we consider a superconducting disk with radius $R_o = 2.0\xi$ and thickness $d = 0.1\xi$ with a hole with radius $R_i = 0.5\xi$ in the center. The free energy and the magnetization (after averaging over the superconductor+hole) for such a ring are shown in Fig. 6. The dashed curves give the free energy and the magnetization for the different L states, and the solid curve is the result for the ground state. Figs. 7(a) and 7(b) show the local magnetic field H, Figs. 7(c) and 7(d) the Cooper-pair density $|\Psi|^2$, and Figs. 7(e) and 7(f) the current density j as function of the radial position ρ for such a ring at the L states and magnetic fields as indicated by the

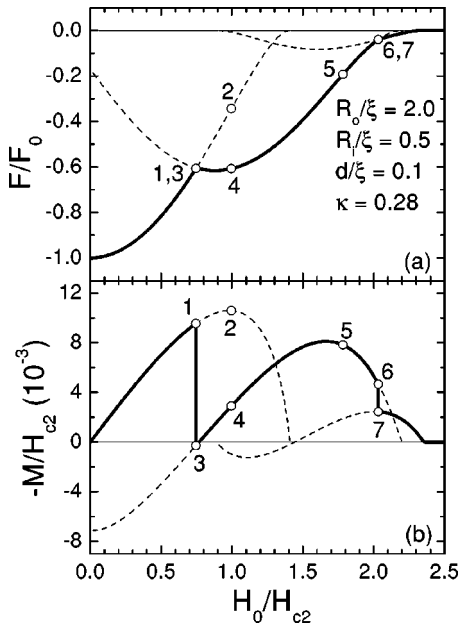

FIG. 6. The free energy (a) and the magnetization after averaging over the superconductor+hole (b) as a function of the applied magnetic field for a superconducting disk with outer radius $R_o=2.0\xi$ and thickness $d=0.1\xi$ with a hole with radius $R_i=0.5\xi$ in the center ($\kappa=0.28$) for the different L states (dashed curves) and for the ground state (solid curves). The open circles are at: (1) $L=0$, $H_0/H_{c2}=0.745$; (2) $L=0$, $H_0/H_{c2}=0.995$; (3) $L=1$, $H_0/H_{c2}=0.745$; (4) $L=1$, $H_0/H_{c2}=0.995$; (5) $L=1$, $H_0/H_{c2}=1.7825$; (6) $L=1$, $H_0/H_{c2}=2.0325$; and (7) $L=2$, $H_0/H_{c2}=2.0325$.

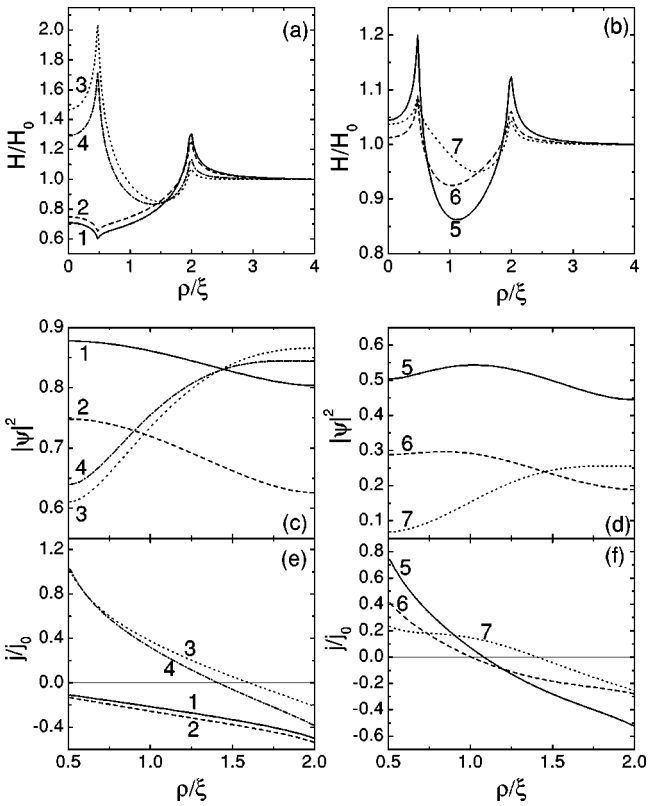

FIG. 7. The local magnetic field H (a,b), the Cooper-pair density $|\Psi|^2$ (c,d) and the current density j (e,f) for the situations indicated by the open circles in Fig. 6 as a function of the radial position ρ for a superconducting disk with radius $R_o=2.0\xi$ and thickness $d=0.1\xi$ with a hole with radius $R_i=0.5\xi$ in the center ($\kappa=0.28$).

open circles in Figs. 6(a) and 6(b).

For low magnetic field, the system is in the $L=0$ state, i.e., the Meissner state, and the flux trapped in the hole is considerably suppressed. Hence, the local magnetic field inside the hole is lower than the external applied magnetic field as is shown in Fig. 7(a) by curves 1 and 2. Please notice that the plotted magnetic field is scaled by the applied field H_0. In the $L=0$ state the superconductor expels the magnetic field by inducing a supercurrent, which tries to compensate the applied magnetic field in the superconductor and inside the hole. This is called the diamagnetic Meissner effect. As long as L equals zero, the induced current has only to compensate the magnetic field at the outside of the ring and, therefore, the current flows in the whole superconducting material in the same direction and the size increases with increasing field. This is clearly shown in Fig. 7(e) by curves 1 and 2 where the current density j becomes more negative for increasing H_0/H_{c2}. Notice also that the current density is more negative at the outside than at the inside of the superconducting ring, which leads to a stronger depression of the Cooper-pair density at the outer edge as compared to the inner edge of the ring [see curves 1 and 2 in Fig. 7(c)].

At $H_0/H_{c2}=0.745$, the ground state changes from the $L=0$ to the $L=1$ state [see Fig. 6(a)]. Suddenly more flux becomes trapped in the hole [compare curve 1 with curve 3 in Fig. 7(a)], the local magnetic field inside the hole increases and becomes larger than the external magnetic field H_0. In the $L=1$ state, there is a sharp peak in the magnetic field at the inner boundary because of demagnetization effects. Consequently, more current is needed to compensate the magnetic field near the inner boundary than near the outer boundary [see curve 3 in Fig. 7(e)]. The sign of the current near the inner boundary becomes positive (the current direction reverses), but the sign of the current near the outer boundary does not change. This can be explained as follows: Near the inner boundary ($\rho\gtrsim 1.0\xi$) the magnetic field is compressed into the hole (paramagnetic effect), while near the outer boundary ($\rho\lesssim 2.0\xi$) the magnetic field is expelled to the insulating environment (diamagnetic effect). The sign reversal of j occurs at $\rho=\rho^*$ and later we will show that the flux through the circular area with radius ρ^* is exactly quantized. At the $L=0$ to the $L=1$ transition the maximum in the Cooper-pair density [compare curves 1 and 3 in Fig. 7(c)] shifts from $\rho=R_i$ to $\rho=R_o$. Further increasing the external field increases the Cooper-pair density near the inner boundary initially [compare curves 3 and 4 in Fig. 7(c)], because the flux in the hole has to be compressed less. The point ρ^*, where $j=0$, shifts towards the inner boundary of the ring. Further increasing the external magnetic field, the Cooper-pair density starts to decrease [see curves 5 and 6 in Fig. 7(d)] and attains its maximum near the inner boundary. The current near the inner boundary becomes less positive [see curves 5 and 6 in Fig. 7(f)], i.e., less shielding of the external magnetic field inside the hole [see curves 5 and 6 in Fig. 7(b)], and near the outer boundary j becomes less negative, which shields the magnetic field from the superconductor+hole. Thus at the outer edge the local magnetic field has a local maximum, which decreases with applied magnetic field H_0.

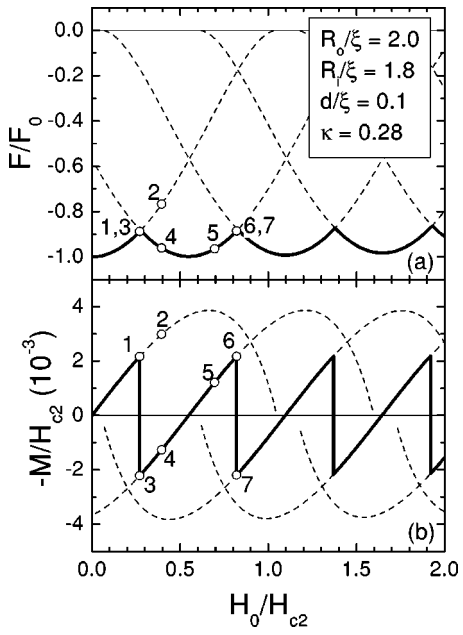

FIG. 8. The free energy (a) and the magnetization after averaging over the superconductor+hole (b) as a function of the applied magnetic field for a superconducting disk with outer radius $R_o = 2.0\xi$ and thickness $d = 0.1\xi$ with a hole with radius $R_i = 1.8\xi$ in the center ($\kappa = 0.28$) for the different L states (dashed curves) and for the ground state (solid curves). The open circles are at: (1) $L = 0$, $H_0/H_{c2} = 0.27$; (2) $L = 0$, $H_0/H_{c2} = 0.395$; (3) $L = 1$, $H_0/H_{c2} = 0.27$; (4) $L = 1$, $H_0/H_{c2} = 0.395$; (5) $L = 1$, $H_0/H_{c2} = 0.695$; (6) $L = 1$, $H_0/H_{c2} = 0.82$; and (7) $L = 2$, $H_0/H_{c2} = 0.82$.

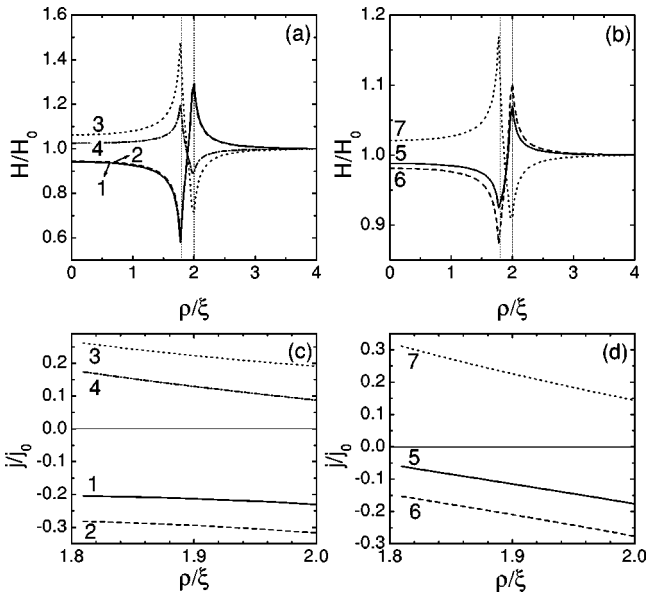

FIG. 9. The local magnetic field H (a,b) and the current density j (c,d) for the situations indicated by the open circles in Fig. 8 as a function of the radial position ρ for a superconducting disk with radius $R_o = 2.0\xi$ and thickness $d = 0.1\xi$ with a hole with radius $R_i = 1.8\xi$ in the center ($\kappa = 0.28$).

At $H_0/H_{c2} \approx 2.0325$, the ground state changes from the $L = 1$ state to the $L = 2$ state and extra flux is trapped in the hole. The changes in the magnetic field distribution, the Cooper-pair density and the current density are analogous to the changes at the first transition. For example, the magnetic field inside the hole increases compared to the external magnetic field [curve 7 in Fig. 7(b)], the radius ρ^* increases substantially [curve 7 in Fig. 7(f)] and the maximum in the Cooper-pair density shifts to the outer boundary [curve 7 in Fig. 7(d)].

For $R_i \ll R_o$ and $L > 0$, the superconducting state consists of a combination of the paramagnetic and the diamagnetic Meissner state, like for a disk. For $R_i \lesssim R_o$ we expect that the sample behaves like a loop and, hence, the superconducting state is a pure paramagnetic Meissner state or a pure diamagnetic Meissner state.

We consider a superconducting disk with radius $R_o = 2.0\xi$ and thickness $d = 0.1\xi$ with a hole with radius $R_i = 1.8\xi$ in the center. The free energy and the magnetization (after averaging over the superconductor+hole) for such a ring are shown in Fig. 8. The dashed curves give the free energy and the magnetization for the different L states, and the solid curve is the result for the ground state. Figures 9(a) and 9(b) show the local magnetic field H, and Figs. 9(c) and 9(d) the current density j as function of the radial position ρ for such a ring at the L states and magnetic fields as indicated by the open circles in Figs. 8(a) and 8(b). The Cooper-pair density has almost no structure and is practically constant over the ring and will, therefore, not be shown.

For $L = 0$, the situation is the same as for $R_i \ll R_o$. The magnetic field is expelled from the superconductor and the hole to the outside of the system, i.e., diamagnetic Meissner effect. The current flows in the whole superconducting material in the same direction [curves 1 and 2 in Fig. 9(a)] and the size increases with increasing external field H_0 [curves 1 and 2 in Fig. 9(c)]. At $H_0/H_{c2} = 0.27$, the ground state changes from the $L = 0$ state to the $L = 1$ state and suddenly more flux is trapped in the hole. The local magnetic field inside the hole becomes larger than the external field H_0 and there is a sharp peak near the inner boundary [curves 3 and 4 in Fig. 9(a)]. In contrast to the situation for $R_i \ll R_o$, there is no peak near the outer boundary, which means that the magnetic field is only expelled to the hole, i.e., paramagnetic Meissner effect. The induced current flows in the reverse direction in the whole superconductor [curves 3 and 4 in Fig. 9(c)]. For increasing external magnetic field, the magnetic field inside the hole, the height of the demagnetization peak, and hence the size of the current decrease [see curves 3 and 4 in Figs. 9(a) and 9(c)]. Further increasing the field, the superconducting state transforms into a diamagnetic Meissner state. The magnetic field is now expelled to the outside of the sample [curves 5 and 6 in Fig. 9(b)] and the direction of the current is the same everywhere in the ring [curves 5 and 6 in Fig. 9(d)]. At $H_0/H_{c2} = 0.82$, the ground state changes from the $L = 1$ state to the $L = 2$ state. The changes in the magnetic field distribution [see curve 7 in Fig. 9(b)] and the current density [see curve 7 in Fig. 9(c)] are analogous to the changes at the first transition. The diamagnetic state transforms into a paramagnetic state.

For a narrow ring with finite width, the superconductor is in the paramagnetic or the diamagnetic Meissner state, like for a superconducting loop. Contrary to this infinitely narrow ring case, for narrow finite width rings the superconducting state can also consist of a combination of these two states, i.e., the direction of the supercurrent in the inner part of the

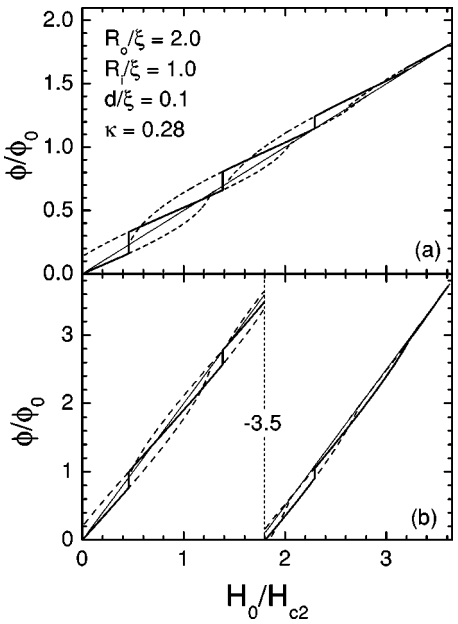

FIG. 10. The flux through (a) the hole and (b) the superconductor+the hole as a function of the applied magnetic field H_0 for a superconducting disk with radius $R_o=2.0\xi$ and thickness $d=0.1\xi$ with a hole in the center with radius $R_i=1.0\xi$. The dashed curves show the flux for the different L states, the solid curve for the ground state. The thin solid line is the flux in the absence of superconductivity.

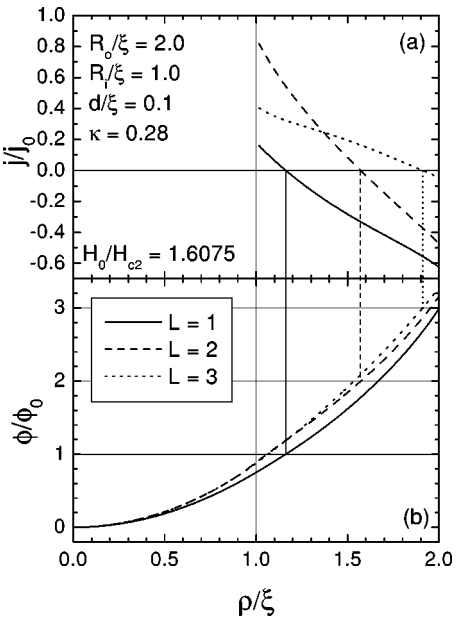

FIG. 11. The current density (a) and the flux (b) as a function of the radial position ρ for a superconducting ring with $R_o=2.0\xi$, $R_i=1.0\xi$, $d=0.1\xi$, and $\kappa=0.28$ for $L=1$ (solid curves), $L=2$ (dashed curves), and $L=3$ (dotted curves) at an applied magnetic field $H_0/H_{c2}=1.6075$.

ring is opposite to the outer part.

Now we will investigate the flux quantization in the fat ring. Figure 10 shows the flux through the hole (a) and through the superconductor+hole (b) as function of the applied magnetic field H_0 for a superconducting disk with radius $R_o=2.0\xi$ and thickness $d=0.1\xi$ with a hole in the center with radius $R_i=1.0\xi$. The dashed curves show the flux for the different L states, the solid curve for the ground state, and the thin solid line is the flux through the hole if the sample is in the normal state. It is apparent that the flux through the hole (or through the superconducting ring +hole) is *not quantized* [see Fig. 10(a)]. At $H_0/H_{c2}=0.4575$ suddenly more flux enters the hole and the ground state changes from the $L=0$ state to the $L=1$ state. At this transition also the flux increase through the hole is not equal to one flux quantum ϕ_0. It is generally believed that the flux through a superconducting ring is quantized. But as was shown in Ref. 23 this is even no longer true for hollow cylinders when the penetration length is larger than the thickness of the cylinder wall. The present result is a generalization of this observation to mesoscopic ring structures. Note that for the case of Fig. 10 the penetration length is $\lambda/\xi=0.28$ and the effective penetration length $\Lambda/\xi=0.78$ is comparable to the width of the ring $(R_o-R_i)/\xi=1.0$.

For $L>0$, the superconducting current equals zero at a certain ''effective'' radial position $\rho=\rho^*$. It is the flux through the circular area with radius ρ^*, which is quantized and not necessarily the flux through the hole of our disk. Following Ref. 13 we integrate the supercurrent j over a closed contour C lying entirely inside the superconducting material, which embraces the opening, one finds

$$\oint_C \left(\frac{4\pi}{c}\kappa^2\xi^2\vec{j}+\vec{A}\right)\cdot d\vec{l}=L\phi_0. \tag{7}$$

Starting from the definition of flux and using Stokes' theorem, the flux can be written as

$$\phi=\int \vec{H}\cdot d\vec{S}=\int rot\vec{A}\cdot d\vec{S}=\oint_C \vec{A}\cdot d\vec{l}. \tag{8}$$

If the contour C is chosen in such a way that the current $j=j_S=0$ on this contour, then the flux through the surface area bounded by this contour is quantized

$$\phi=\oint_C \vec{A}\cdot d\vec{l}=L\phi_0. \tag{9}$$

To demonstrate that this is indeed true we show in Fig. 11(a) the current density as a function of the radial position ρ and in Fig. 11(b) the flux through a circular area with radius ρ for a superconducting disk with radius $R_o=2.0\xi$ and thickness $d=0.1\xi$ with a hole in the center with radius $R_i=1.0\xi$ in the presence of an external magnetic field $H_0/H_{c2}=1.6075$ for the case of three different giant vortex states; i.e., $L=1,2,3$. In the $L=1$ state, the current density equals zero at a distance $\rho^*/\xi\approx1.16$ from the center and the flux through an area with this radius is exactly equal to one flux quantum ϕ_0. For $L=2$ and $L=3$, the current density j equals zero at $\rho^*/\xi\approx1.56$ and 1.91, respectively, and the flux through the area with this radius ρ^* is exactly equal to $2\phi_0$ and $3\phi_0$, respectively. We find that ρ^* depends on the external applied magnetic field and on the value of L, contrary to the results of Arutunyan and Zharkov,[13,14] who found that the effective radius ρ^* is approximately equal to the geometric mean square of the inner radius R_i and the outer radius R_o of the cylinder; i.e., $\rho^*=(R_iR_o)^{1/2}$, which for the

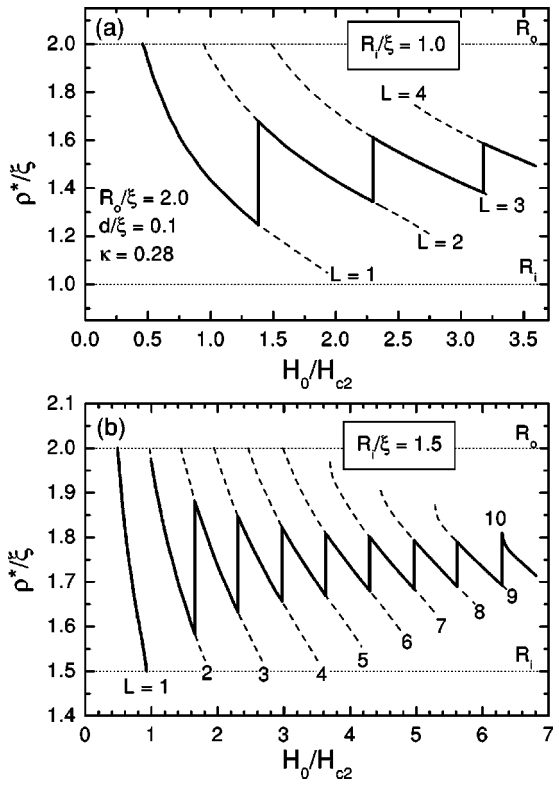

FIG. 12. The dependence of the effective radius ρ^* as function of the applied magnetic field for a superconducting disk with radius $R_o=2.0\xi$ and thickness $d=0.1\xi$ with a hole in the center with radius $R_i=1.0\xi$ (a), and $R_i=1.5\xi$ (b). The dashed curves show ρ^* for the different L states and the solid curve is for the ground state.

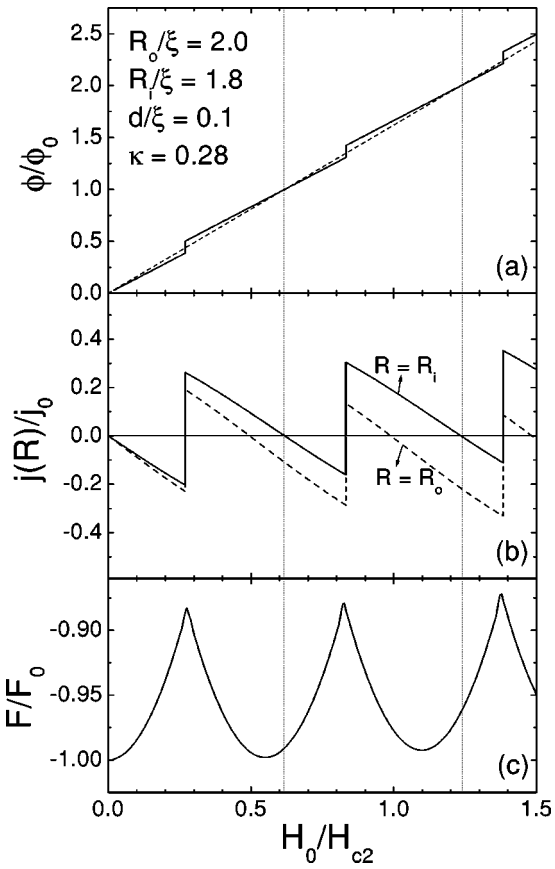

FIG. 13. (a) The flux through the hole of the ring as function of the applied magnetic field. The thin dashed line is the applied flux. (b) The current at the inner side (solid curve) and at the outer side (dashed curve) of the ring, and (c) the free energy of the ground state as function of the applied magnetic field.

case of Fig. 12(a) would give $\rho^*=1.41\xi$. The results of Refs. 13 and 14 were obtained within the London limit. The dependence of ρ^* as function of the applied magnetic field is shown in Fig. 12(a). The dashed curves give the ρ^* of the different L states. For increasing magnetic field and fixed L, the value of ρ^* decreases, i.e., the ''critical'' radius moves towards the inner boundary. The solid curve gives ρ^* for the ground state. At the $L\rightarrow L+1$ transitions, ρ^* jumps over a considerable distance towards the outside of the superconducting ring, the size of the jumps decreases with increasing L. The dotted lines in the figure give the two boundaries of the superconducting ring: the outer boundary $R_o=2.0\xi$ and the inner boundary $R_i=1.0\xi$. Remark that in Fig. 12 there is no ρ^* given for the $L=0$ state, because only the external magnetic field has to be compensated so that the current has the same sign everywhere inside the ring and there exists no ρ^*. In Fig. 12(b) we repeated this calculation for a hole with radius $R_i=1.5\xi$, where superconductivity remains to higher magnetic fields and many more $L\rightarrow L+1$ transitions are possible. The result of Refs. 13 and 14 gives in this case $\rho^*=1.73\xi$. Remark that the results for the $L=1$ and the $L=2$ states are not connected. The reason is that just before the $L=1\rightarrow L=2$ transition the critical current for the $L=1$ state is strictly positive in the whole ring and hence ρ^* is not defined. Notice that the results in Figs. 12(a) and 12(b) oscillate around the average value $\rho^*=\sqrt{R_iR_o}$ as given by Refs. 13 and 14.

For even narrower rings the current in the ring is mostly diamagnetic or paramagnetic and the region in magnetic field over which both directions of current occur in the ring becomes very narrow. This is illustrated in Fig. 13 for a ring with outer radius $R_o=2.0\xi$ and inner radius $R_i=1.8\xi$. We plot in Fig. 13(a) the flux through the hole, which becomes very close to the external flux, i.e., the flux without any superconductor. In Fig. 13(b) the value of the current at the inner and the outer side of the ring is shown, which illustrates nicely that over large ranges of the magnetic field the current in the ring flows in one direction. The free energy becomes minimum [see Fig. 13(c)] at a magnetic field where the current in the rings flows in both directions.

IV. LARGE RINGS: THE MULTIVORTEX STATE

Until now, we considered only small rings. In such rings, the confinement effect dominates and we found that only the giant vortex states are stable and possible multivortex states have always larger energies if they exist. Now we will consider larger superconducting disks in which multivortex states can nucleate for certain magnetic fields. As an example we take a fat ring with outer radius $R_o=4.0\xi$, thickness $d=0.005\xi$, $\kappa=0.28$ and for different values of the inner radius. Figure 14(a) shows the free energy for such a ring with inner radius $R_i=0.4\xi$ as a function of the applied magnetic field H_0. The different giant vortex states are given by the thin solid curves and the multivortex state by the thick solid

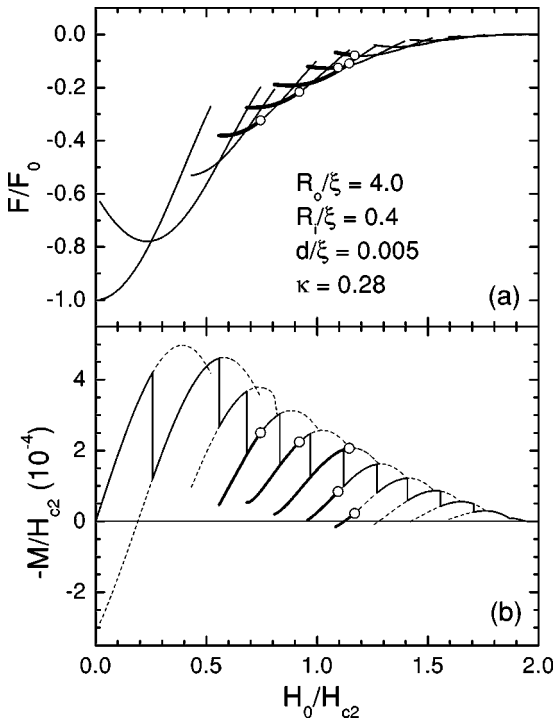

FIG. 14. (a) The free energy as function of the applied magnetic field for a superconducting ring with $R_o=2.0\xi$, $R_i=0.4\xi$, $d=0.005\xi$, and $\kappa=0.28$. The different giant vortex states are shown by the thin solid curves and the multivortex states by the thick solid curves. (b) The magnetization for the same sample after averaging over the superconducting ring only. The different L states are given by the dashed curves, the ground state by the thin solid curves, and the multivortex states by the thick solid curves. The transitions from multivortex state to giant vortex state are indicated by the open circles.

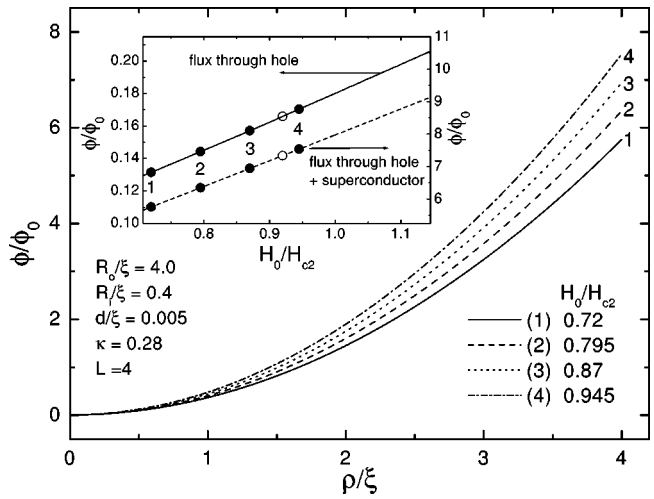

FIG. 15. The flux ϕ through a circular area of radius ρ for different values of the applied magnetic field; H_0. Curves 1, 2, 3, and 4 give the results for $H_0/H_{c2}=0.72$ (1), 0.795 (2), 0.87 (3) (i.e., multivortex states), and 0.945 (4) (i.e., giant vortex state), respectively. The inset shows the flux through the hole with radius $R_i=0.4\xi$ and through the superconductor+hole as a function of the applied magnetic field for a fixed value of the winding number, i.e., $L=4$. The solid circles indicate the magnetic fields considered in the main figure and the open circles indicate the transition from multivortex to giant vortex state.

curves. The open circles indicate the transitions from the multivortex state to the giant vortex state. In this ring, multivortex states exist with winding number $L=3$ up to 7. For $L=3,4,5$, multivortices occur both as metastable states as well as in the ground state, while for $L=6,7$ they are only found in the metastable state. Notice there is no discontinuity in the free energy at the transitions from the multivortex state to the giant vortex state for fixed winding number L. Figure 14(b) shows the magnetization M for this ring as a function of H_0 after averaging the field H over the superconducting ring (without the hole). The dashed curves give the results for the different L states, the thin solid curve for the ground state, the thick solid curves for the multivortex states, and the open circles indicate the transition from the multivortex state to the giant vortex states. Notice that the latter transitions are smooth, there are no discontinuities in the magnetization.

Now, we investigate the flux ϕ through the hole for the $L=4$ multivortex and giant vortex state for the case of the above ring. Figure 15 shows the flux ϕ through a circular area of radius ρ for different values of the applied magnetic field H_0. Curves 1, 2, 3, and 4 are the results for $H_0/H_{c2}=0.72$, 0.795, 0.87 (i.e., multivortex states), and 0.945 (i.e., giant vortex state), respectively. There is no qualitative difference between the 4 curves, i.e., no qualitative difference between the multivortex states and the giant vortex state. In the inset, we show the flux through the hole with radius $R_i=0.4\xi$ and through the superconductor+hole as a function of the applied magnetic field for a fixed value of the winding number, i.e., $L=4$. The solid circles indicate the magnetic fields considered in the main figure and the open circle indicates the position of the transition from multivortex state to giant vortex state. The slope of the curves increases slightly at the applied magnetic field, where there is a transition from the multivortex state to the giant vortex state. This agrees with the result for a disk[6] that the giant↔multivortex transition is a second-order phase transition.

The Cooper-pair density $|\psi|^2$ for the previous four configurations is shown in Fig. 16. The darker the region, the larger the density and thus vortices are given by white regions. At the magnetic field $H_0/H_{c2}=0.72$ [Fig. 16(a)] we see clearly three multivortices. With increasing magnetic field, these multivortices start to overlap and move to the center [Figs. 16(b) and 16(c)] and finally they combine to one giant vortex in the center [Fig. 16(d)]. Please notice that a theory based on the London limit will not be able to give such a complicated behavior, because in such a theory vortices are rather pointlike objects.

The free energies of the different vortex configurations were calculated for different values of the hole radius, which we varied from $R_i=0$ to $R_i=3.6\xi$. From these results we constructed an equilibrium vortex phase diagram. First, we assumed axial symmetry, where only giant vortex states occur and the order parameter is given by $\Psi(\vec{\rho})=F(\rho)e^{iL\theta}$. In the phase diagram (Fig. 17) the solid curves separate the regions with different number of vortices (different L states). In the limit $R_i\rightarrow 0$ we find the previous results of Ref. 6 for a superconducting disk. The radius of the giant vortex R_L in the center of the disk increases with increasing L, because it has to accommodate more flux, i.e., $R_L/\xi\sim\sqrt{L/(H_0/H_{c2})}$.

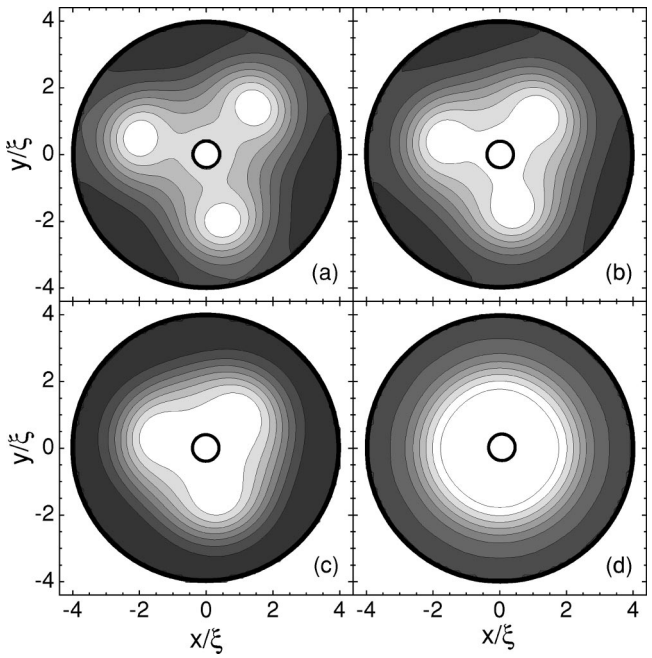

FIG. 16. The Cooper-pair density corresponding to the four situations of Fig. 15: $H_0/H_{c2}=0.72$ (a); $H_0/H_{c2}=0.795$ (b); $H_0/H_{c2}=0.87$ (c); and $H_0/H_{c2}=0.945$ (d). Dark regions indicate high density, light regions low density. The thick circles indicate the inner and the outer edge of the ring.

Hence, if we make a little hole in the center of the disk, this will not influence the $L\rightarrow L+1$ transitions as long as $R_i \ll R_L$ as is apparent from Fig. 17. For sufficient large hole radius R_i, the hole starts to influence the giant vortex configuration and the magnetic field needed to induce the $L\rightarrow L+1$ transition increases. For example, the transition field from the $L=7$ state to the $L=8$ state reaches its maximum for a hole radius $R_i\approx 2.0\xi$, which occurs for $H_0/H_{c2}\approx 1.5$.

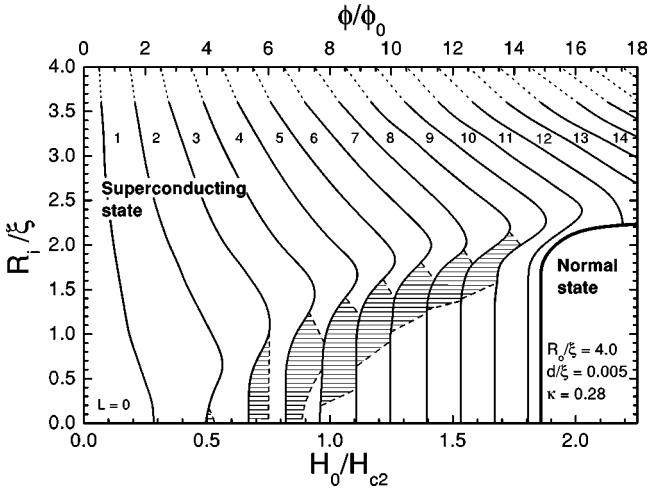

FIG. 17. Equilibrium vortex phase diagram for a superconducting disk with radius $R_o=4.0\xi$, thickness $d=0.005\xi$ with a hole with radius R_i in the center. The solid curves show the transitions between the different L states, the thick solid curve shows the superconducting/normal transition and the dotted lines connect the results for $R_i=3.6\xi$ with the results in the limit $R_i\rightarrow R_o$. The shaded regions indicate the multivortex states and the dashed curves separate the multivortex states from the giant vortex states.

The above rough estimate gives $R_L/\xi\sim 2.16$, which is very close to $R_i/\xi\sim 2.0$. Further increasing R_i, the hole becomes so large that more and more flux is trapped inside the hole, and consequently a smaller field is needed to induce the $L\rightarrow L+1$ transition. Because of finite grid size, we were limited to $R_i\leqslant 3.6\xi$. The results we find for $R_i=3.6\xi$ are extrapolated to $\phi=(L+1/2)\phi_0$ for $R_i=R_o$. The thick curve in Fig. 17 gives the superconducting/normal transition. For low values of R_i, this critical magnetic field is independent of R_i, because the hole is smaller than the giant vortex state in the center and hence the hole does not influence the superconducting properties near the superconducting/normal transition. For $R_i\gtrsim 2.0\xi$, this field starts to increase drastically. Therefore, more and more L states appear. In the limit $R_i\rightarrow R_o$, the critical magnetic field is infinite and there are an infinite number of L states possible, which is a consequence of the enhancement of surface superconductivity for very small superconducting samples.[22]

Next, we consider the general situation where the order parameter is allowed to be a mixture of different giant vortex states and thus we no longer assume axial symmetry of the superconducting wave function. We found that the transitions between the different L states are not influenced by this generalization, but that for certain magnetic fields the ground state is given by the multivortex state instead of the giant vortex state. In Fig. 17 the shaded regions correspond to the multivortex states and the dashed curves are the boundaries between the multivortex and the giant vortex states. For $L=1$, the single vortex state and the giant vortex state are identical. In the limit $R_i\rightarrow 0$, the previous results of Ref. 6 for a superconducting disk are recovered. For increasing hole radius R_i, the $L=2$ multivortex state disappears as a ground state for $R_i>0.15\xi$. If R_i is further increased, the ground state for $L=5$ up to $L=9$ changes from giant vortex state to multivortex state and again to giant vortex state. For example, for $R_i=2.0\xi$ the multivortex state exists only in the $L=9$ state. Notice that for small R_i the region of multivortex states increases and consequently the hole in the center of the disk stabilizes the multivortex states, at least for $L>2$. For large R_i, i.e., narrow rings, the giant vortex state is the energetic favorable one because confinement effects start to dominate, which impose the circular symmetry on ψ. For fixed hole radius $R_i\leqslant 2.0\xi$ and increasing magnetic field we find always at least one transition from giant vortex state to multivortex state and back to giant vortex state (re-entrant behavior). Remark that the ground state for $L\geqslant 10$ is in the giant vortex state irrespective of the value of the magnetic field. Near the superconducting/normal transition the superconducting ring is in the giant vortex state because now superconductivity exists only near the edge of the sample and consequently the superconducting state will have the same symmetry as the outer edge of the ring and thus it will be circular symmetric.

Finally, for $L\geqslant 3$ the multivortex state not necessarily consists of L vortices in the superconducting material. Often they consist of a combination of a big vortex trapped in the hole and some multivortices in the superconducting material. This is clearly shown in Fig. 18, where a contour plot of the local magnetic field is given for a superconducting disk with radius $R_o=4.0\xi$ and thickness $d=0.005\xi$ with a hole in the center with radius $R_i=0.6\xi$ [Fig. 18(a)] and $R_i=1.0\xi$ [Fig.

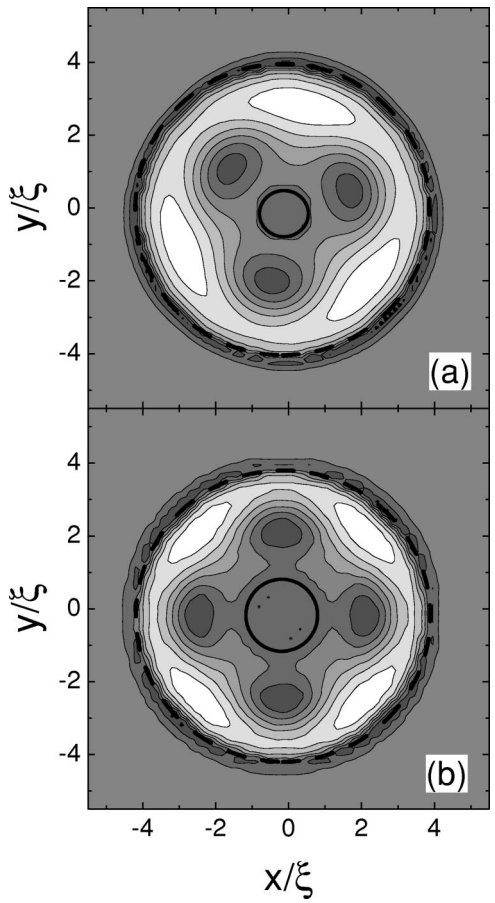

FIG. 18. Contour plot of the local magnetic field for a superconducting disk with radius $R_o=4.0\xi$ and thickness $d=0.005\xi$ ($\kappa=0.28$) with a hole in the center with (a) radius $R_i=0.6\xi$ at $H_0/H_{c2}=0.895$ for $L=4$; and (b) radius $R_i=1.0\xi$ at $H_0/H_{c2}=1.145$ for $L=6$. The dashed thick circle is the outer radius, the small solid thick circle the inner radius. Low magnetic fields are given by light regions and dark regions indicate higher magnetic fields.

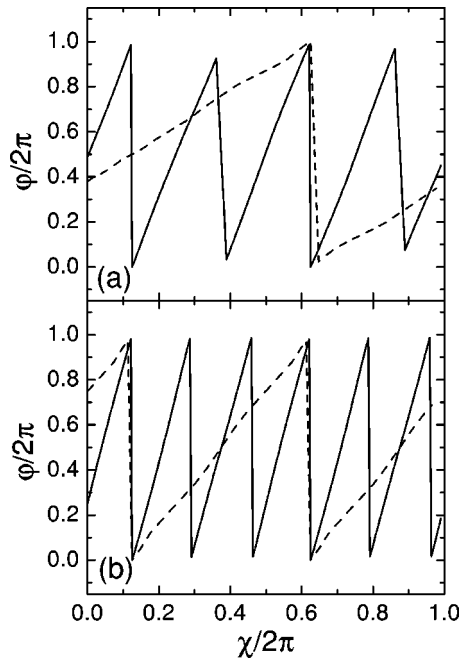

FIG. 19. The phase φ of the order parameter calculated on a circle $\mathbf{r}\rightarrow Ce^{i\chi}$ as a function of the angle χ for a superconducting ring with $R_o=4.0\xi$, $d=0.005\xi$, and $\kappa=0.28$; (a) $R_i=0.6\xi$, $H_0/H_{c2}=0.895$, $L=4$, and $C=3.95\xi$ (solid curve) and $C=0.7\xi$ (dashed curve); (b) $R_i=1.0\xi$, $H_0/H_{c2}=1.145$, $L=6$, and $C=3.95\xi$ (solid curve) and $C=1.2\xi$ (dashed curve).

18(b)]. As usual we took $\kappa=0.28$. The dashed thick circle is the outer radius, while the small solid black circle is the inner radius of the ring. Low magnetic fields are given by light regions and darker regions indicate higher magnetic fields. In this way, multivortices in the superconducting area are dark spots. In Fig. 18(a) the local magnetic field is shown for an applied magnetic field $H_0/H_{c2}=0.895$. Although the winding number is $L=4$, there are only 3 vortices in the superconducting material and one vortex appears in the hole in the center of the disk. This is clearly shown in Fig. 19(a), where the phase φ of the order parameter is shown along different circular loops $\vec{r}\rightarrow Ce^{i\chi}$ inside the superconductor. The solid curve gives the phase near the outer edge of the ring ($C=3.95\xi$) and the dashed curve near the inner edge of the ring ($C=0.7\xi$). When encircling the ring, the phase difference $\Delta\varphi$ in the first case is 4 times 2π, while in the second case it is $\Delta\varphi=1\times2\pi$. The phase difference is always given by $\Delta\varphi=L\times2\pi$, with L the winding number. In Fig. 18(b) a contour plot of the local magnetic field is shown for a ring with $R_i=1.0\xi$, which leads to $L=6$ at $H_0/H_{c2}=1.145$. Only 4 vortices are in the superconducting material and one giant vortex in the center (partially in the hole) with $L=2$. Fig. 19(b) shows the phase φ of the order parameter for $C=3.95\xi$ (solid curve) and 1.2ξ (dashed curve), where the phase differences are $\Delta\varphi=6\times2\pi$ and $2\times2\pi$, respectively. Notice that the flux ϕ through the hole equals $\phi\approx0.19\phi_0$ for the case of Fig. 18(a) and $\phi\approx0.36\phi_0$ for the case of Fig. 18(b) and is thus not equal to a multiple of the flux quantum ϕ_0.

V. NONSYMMETRIC GEOMETRY

So far, we investigated the influence of the size of the hole on the vortex configuration for superconducting rings of different sizes. We found that for small rings, only the axially symmetrical situation occurs, i.e., the giant vortex states. For large rings the multivortex state can be stabilized for certain values of the magnetic field. In the next step, we purposely break the axial symmetry by moving the hole away from the center of the superconducting disk over a distance a.

As an example, we consider a superconducting disk with radius $R_o=2.0\xi$ and thickness $d=0.005\xi$ with a hole with radius $R_i=0.5\xi$ moved over a distance $a=0.6\xi$ in the x-direction. Figure 20 shows the free energy and magnetization (defined as the field expelled from the superconducting ring without the hole) as function of the magnetic field. The solid curve indicates the ground state, while the dashed curves indicate the metastable states for increasing and decreasing field. The vertically dotted lines separate the regions with different winding number L. Notice that hysteresis is only found for the first transition from the $L=0$ to the $L=1$ state and not for the higher transitions which are continuous. At the transition from the $L=1$ state to the $L=2$

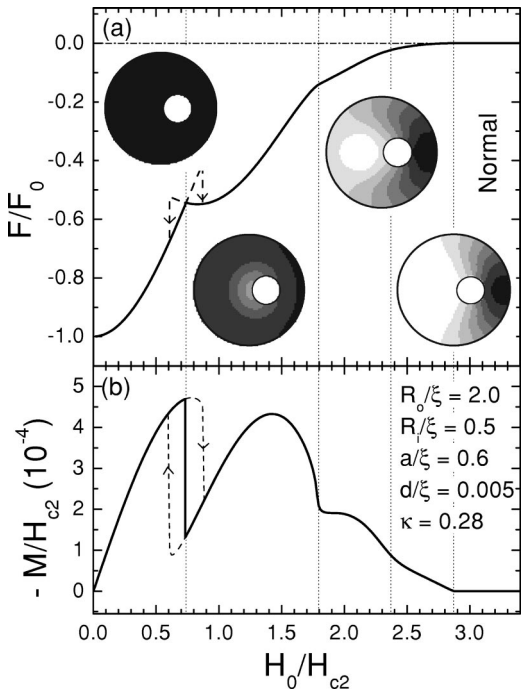

FIG. 20. The free energy (a) and magnetization after averaging over the superconducting ring only (b) as function of the applied magnetic field for a superconducting disk with radius $R_o=2.0\xi$ and thickness $d=0.005\xi$ with a hole with radius $R_i=0.5\xi$ moved over a distance $a=0.6\xi$ in the x-direction. The solid curve indicates the ground state, the dashed curve the results for increasing and decreasing field. The vertically dotted lines separate the regions with different vorticity L. The insets show the Cooper-pair density at magnetic field $H_0/H_{c2}=0.145$, 1.02, 2.145, and 2.52, where the ground state is given by a state with $L=0,1,2,3$, respectively. High Cooper-pair density is given by dark regions, while light regions indicate low Cooper-pair density.

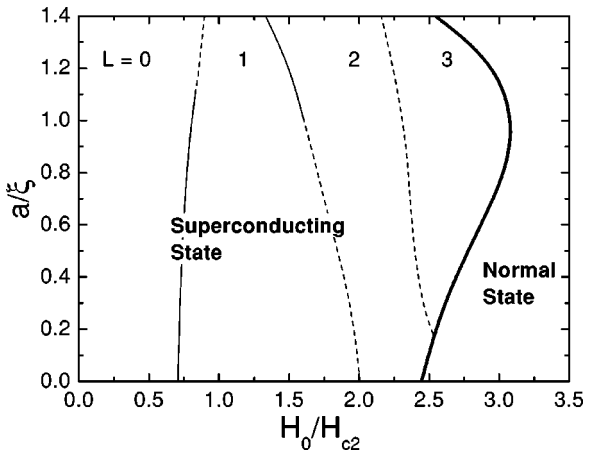

FIG. 21. The relation between the displacement a and the transition magnetic fields for a superconducting ring with $R_0/\xi=2.0$, $d/\xi=0.005$, $R_i/\xi=0.5$, and $\kappa=0.28$. The thin solid curves give the $L\rightarrow L+1$ transitions when it corresponds to a first-order phase transition while a dashed curve is used when it is continuous. The thick solid curve is the superconducting/normal transition.

state and further to the $L=3$ state, the free energy and the magnetization vary smoothly [see Figs. 20(a) and 20(b)]. In the insets of Fig. 20(a), we show the Cooper-pair density for such a sample at magnetic field $H_0/H_{c2}=0.145$, 1.02, 2.145, and 2.52, respectively, where the ground state is given by a state with $L=0,1,2,3$, respectively. High Cooper-pair density is given by dark regions, while light regions indicate low Cooper-pair density. For $H_0/H_{c2}=0.145$, we find a high Cooper-pair density in the entire superconducting ring. There is almost no flux trapped in the circular area with radius smaller than R_o. After the first transition at $H_0/H_{c2}\approx 0.75$, suddenly more flux is trapped in the hole which substantially lowers the Cooper-pair density in the superconductor. Notice that the trapped flux tries to restore the circular symmetry in the Cooper-pair density and that the density of the superconducting condensate is largest in the narrowest region of the superconductor. The next inset shows the Cooper-pair density of the $L=2$ state, where an additional vortex appears. Some flux is passing through the hole (i.e., winding number is one around the hole), while one flux line is passing through the superconducting ring and a local vortex (the normal region with zero Cooper-pair density) is created. In the $L=3$ state superconductivity is destroyed in part of the sample, which contains flux with winding number $L=2$ and the rest of the flux passes through the hole. Hence, by breaking the circular symmetry of the system, multivortex states are stabilized. Remember that for the corresponding symmetric system, i.e., $a=0$, only giant vortex states were found.

Having the magnetic fields for the different $L\rightarrow L+1$ transitions for superconducting rings with different positions of the hole, i.e., different values of a, we constructed the phase diagram shown in Fig. 21. The thin curves (solid curves when the magnetization is discontinuous and dashed curves when the magnetization is continuous) indicate the magnetic field at which the transition from the L-state to the $L+1$-state occurs, while the thick solid curve gives the superconducting/normal transition.

In order to show that the stabilization of the multivortex state due to an off-center hole is not peculiar for $R_o=2.0\xi$, we repeated the previous calculation for a larger superconducting disk with radius $R_o=5.0\xi$ and thickness $d=0.005\xi$ containing a hole with radius $R_i=2.0\xi$. In Fig. 22(a) the Cooper-pair density is shown for such a system with the hole in the center, while in Fig. 22(b) the hole is moved away form the center over a distance $a=1.0\xi$ in the negative y direction. The externally applied magnetic field is the same in both cases, $H_0/H_{c2}=0.77$, which gives a winding number $L=4$ and $L=5$ for the ground state of the symmetric and the nonsymmetric geometry, respectively. The assignment of the winding number can be easily checked from Figs. 22(c) and 22(d), which show contour plots of the corresponding phase of the superconducting wavefunction. If the hole is at the center of the disk, the ground state is a giant vortex state. Moving the center of the hole to the position $(x/\xi,y/\xi)=(0,-1)$, two vortices appear in the superconducting material while the hole contains three vortices. Notice that in this case, although the magnetic field is kept the same and the amount of superconducting material is not altered, changing the symmetry of the system alters the winding number.

VI. CONCLUSION

In conclusion, we studied the superconducting state of thin superconducting disks with a hole. The effect of the size and the position of the hole on the vortex configuration was

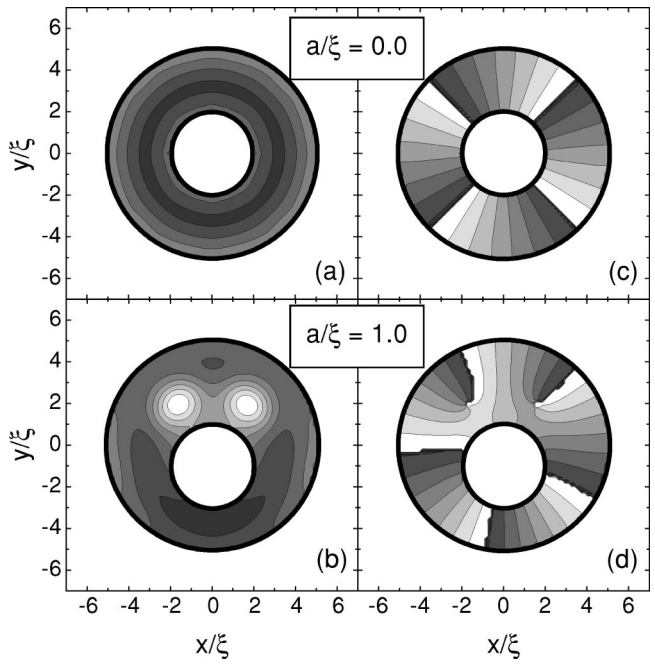

FIG. 22. The Cooper-pair density for a superconducting disk with radius $R_o=5.0\xi$ and thickness $d=0.005\xi$ with a hole with radius $R_i=2.0\xi$ (a) in the center, and (b) moved away from the center over a distance $a=1.0\xi$ in the negative y direction. The applied magnetic field is the same in both cases: $H_0/H_{c2}=0.77$. High Cooper-pair density is given by dark regions, low Cooper-pair density by light regions. The corresponding contour plot of the phase of the superconducting wave function is given in (c) and (d).

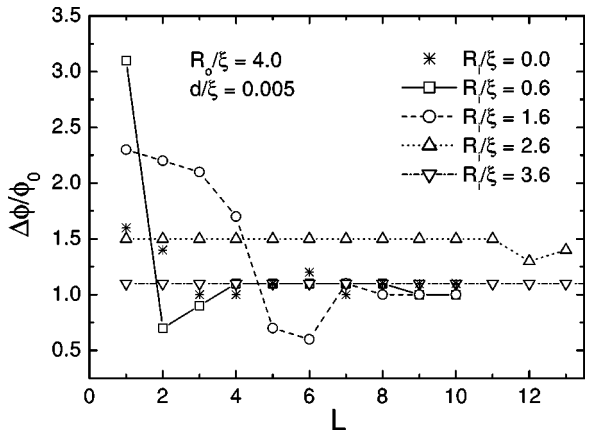

FIG. 23. The flux increase $\Delta\phi=\pi R_o^2\Delta H$ needed to induce the $L\rightarrow L+1$ transition for a superconducting ring with $R_o=4.0\xi$ for different values of the inner radius R_i. The interconnecting lines are a guide to the eye.

investigated. For small superconducting disks with a hole in the center, only giant vortex states exist and for increasing hole radius R_i more and more L states occur before the superconductor becomes normal. For larger superconducting disks with a hole in the center, we found multivortex states in a certain magnetic field range. For certain fixed hole radius, and for increasing magnetic field, the giant vortex state changes into a multivortex state and back into the giant vortex state (re-entrant behavior) before superconductivity is destroyed. Near the superconducting/normal transition and for a narrow superconducting ring (i.e., $R_i\approx R_o$) we always found the giant vortex state as the ground state irrespective of the size, thickness, and width of the ring. The effect of the position of the hole, i.e., decreasing the symmetry of the system, was also investigated. Moving the hole off-center: 1) can transform the $L\rightarrow L+1$ transition into a continuous one, 2) the stability of metastable states is strongly reduced, 3) it favors the multivortex state even for small disks, and 4) the winding number L can increase even at a fixed magnetic field.

The flux through the hole is *not* quantized. We were able to define an effective ring size ρ^* such that inside this ring the flux is exactly quantized. The value of $R_i\leqslant\rho^*\leqslant R_o$ depends on L and is an oscillating function of the magnetic field. For narrow rings it is only possible to define such a ρ^* in narrow ranges of the magnetic field and the flux through the hole is very close to the applied flux. The magnetic fields from the screening currents are too small to substantially modify the flux inside the ring. On the other hand, the magnetic field increment ΔH or the flux increase $\Delta\phi=\pi R_o^2\Delta H$ to induce the $L\rightarrow L+1$ transition is only quantized for narrow rings. This is illustrated in Fig. 23 in case of $R_o=4.0\xi$ for different values of the inner radius. Notice that for $R_i\ll R_o$ we find that $\Delta\phi$ is an oscillating function of L. It is substantially larger than ϕ_0 for small L, it is smaller than ϕ_0 for intermediate L and it approaches ϕ_0 from above for large L. We found earlier that for $R_i\approx R_o$ the flux through $\rho^*=\sqrt{R_iR_o}$ is quantized in ϕ_0 and therefore we expect $\Delta\phi^*=\pi(\rho^*)^2\Delta H=\phi_0$. Our definition of $\Delta\phi$, considers the flux through the superconducting ring+hole which for the condition $\Delta\phi^*=\phi_0$ gives $\Delta\phi/\phi_0\approx 6.67$, 2.5, 1.54, and 1.11 for $R_i/\xi=0.6$, 1.6, 2.6, and 3.6, respectively. These results for $R_i/\xi=2.6$ and 3.6 agree rather well with our numerical results presented in Fig. 23; i.e., $\Delta\phi/\phi_0\approx 1.5$ and 1.1, respectively. The results presented in Fig. 23 agree qualitatively with the recent theoretical results of Bruyndoncx *et al.*,[16] who studied rings in a homogeneous magnetic field.

ACKNOWLEDGMENTS

This work was supported by the Flemish Science Foundation (FWO-Vl), IUAP-VI, and ESF-Vortex Matter. One of us (B.J.B.) was supported by BOF (SFO) (Antwerp). One of us (F.M.P.) acknowledges discussions with J. P. Lindelof.

*Electronic address: peeters@uia.ua.ac.be
†Permanent address: Institute of Theoretical and Applied Mechanics, Russian Academy of Sciences, Novosibirsk 630090, Russia.

[1] W.A. Little and R.D. Parks, Phys. Rev. Lett. **9**, 9 (1962); Phys. Rev. **133**, A97 (1964).
[2] J. Berger and J. Rubinstein, Phys. Rev. Lett. **75**, 320 (1995); Phys. Rev. B **56**, 5124 (1997).
[3] See, e.g., M. Thinkham: *Introduction to Superconductivity* (McGraw-Hill, London, 1975).
[4] V.A. Schweigert and F.M. Peeters, Phys. Rev. B **57**, 13 817 (1998).
[5] P.S. Deo, V.A. Schweigert, F.M. Peeters, and A.K. Geim, Phys. Rev. Lett. **79**, 4653 (1997).
[6] V.A. Schweigert, F.M. Peeters, and P.S. Deo, Phys. Rev. Lett. **81**,

2783 (1998).
[7] P.S. Deo, F.M. Peeters, and V.A. Schweigert, Superlattices Microstruct. **25**, 1195 (1999).
[8] J.J. Palacios, Phys. Rev. B **58**, R5948 (1998); E. Akkermans and K. Mallick, J. Phys. A **32**, 7133 (1999).
[9] G. Dolan, J. Low Temp. Phys. **15**, 133 (1974).
[10] V.V. Moshchalkov, X.G. Qiu, and V. Bruyndoncx, Phys. Rev. B **55**, 11 793 (1997); L. J. Barnes, and H. J. Fink, Phys. Lett. **20**, 583 (1966); Phys. Rev. **149**, 186 (1966); H. J. Fink and A. G. Presson, *ibid.* **151**, 219 (1966).
[11] A. Bezryadin, A. Buzdin, and B. Pannetier, Phys. Rev. B **51**, 3718 (1995).
[12] J. Bardeen, Phys. Rev. Lett. **7**, 162 (1961).
[13] G. F. Zharkov, in *Superconductivity, Superdiamagnetism, Superfluidity*, edited by V. L. Ginzburg (MIR, Moscow, 1987), p. 126.
[14] R.M. Arutynyan and G.F. Zharkov, J. Low Temp. Phys. **52**, 409 (1983); H. J. Fink and V. Gruenfeld, Phys. Rev. B **22**, 2289 (1980) found a different expression for the effective radius. But for the situation of Figs. 12(a) and (b) both results for the effective radius differ by less than 3%.
[15] V.M. Fomin, V.R. Misko, J.T. Devreese, and V.V. Moshchalkov, Phys. Rev. B **58**, 11 703 (1998).
[16] V. Bruyndoncx, L. Van Look, M. Verschuere, and V.V. Moshchalkov, Phys. Rev. B **60**, 10 468 (1999).
[17] J. Berger and J. Rubinstein, Phys. Rev. B **59**, 8896 (1999).
[18] I.V. Schweigert, V.A. Schweigert, and F.M. Peeters, Phys. Rev. B **54**, 10 827 (1996).
[19] R. Kato, Y. Enomoto, and S. Maekawa, Phys. Rev. B **47**, 8016 (1993).
[20] A.K. Geim, I.V. Grigorieva, S.V. Dubonos, J.G.S. Lok, J.C. Maan, A.E. Filippov, and F.M. Peeters, Nature (London) **390**, 259 (1997).
[21] F.M. Peeters and X.Q. Li, Appl. Phys. Lett. **72**, 572 (1998).
[22] V.A. Schweigert and F.M. Peeters, Phys. Rev. B **60**, 3084 (1999); V.M. Fomin, J.T. Devreese, and V.V. Moshchalkov, Europhys. Lett. **42**, 553 (1998); *ibid.* **46**, 118 (1999); A.P. van Gelden, Phys. Rev. Lett. **20**, 1435 (1968).
[23] R.P. Groff and R.D. Parks, Phys. Rev. **176**, 567 (1968).